# Regio- and Stereochemistry of Alkene Expulsion from Ionized *sec*-Alkyl Phenyl Ethers†

**John C. Traeger**

*Department of Chemistry, LaTrobe University, Bundoora, Victoria, Australia*

**Alberto Luna and Jeanine C. Tortajada**

*COS, UMR CNRS 172, Université de Paris VI, boîte 45, 4 place Jussieu,75252 Paris Cedex 05, France*

**Thomas Hellman Morton***

*Department of Chemistry, University of California, Riverside, California 92521-0403*

*Received: September 28, 1998; In Final Form: January 13, 1999*

Photoionization mass spectrometry of isotopically substituted 2-phenoxypropane (iPrOPh), 2-phenoxybutane (sBuOPh), and 3-phenoxypentane (3AmOPh) permits the analysis of branching ratios for competing pathways by which the radical cations expel neutral alkene to yield ionized phenol. Ionization energies (IEs) of 2-phenoxyalkanes do not differ significantly between 2-phenoxypropane and 2-phenoxyoctane and are unaffected by deuterium substitution. IEs for 3-phenoxyalkanes are 0.04 eV lower than for the 2-phenoxyalkanes. Measurements of $PhOD^{\bullet+}$:$PhOH^{\bullet+}$ ratios from deuterated analogues as a function of photon energy lead to a dissection of two mechanisms: direct syn elimination via four-member transition states (which differentiates between stereochemically distinct positions on an adjacent methylene group) and formation of ion−neutral complexes (which affords hydrogen transfer from all positions of the side chain). Syn elimination from ionized sBuOPh partitions among *trans*-2-butene, *cis*-2-butene, and 1-butene in a ratio of approximately 6:5:4, exhibiting no systematic variation with internal energy. The proportion of ion−neutral complex formation for sBuOPh increases with energy, from virtually nil at 9.6 eV to about 20% at 9.81 eV to slightly more than one-half at 11.92 eV. Ion−neutral complexes from sBuOPh yield nearly equal proportions of 1-butene and 2-butenes, with little variation as a function of internal energy, while those from 3AmOPh yield about 80−90% 2-pentenes. DFT calculations confirm the preference for syn elimination from ionized iPrOPh at low internal energies. The computed energy of that transition state agrees with published experimental determinations. Analysis of the electron density using the atoms-in-molecules approach shows that the transition state does not possess cyclic topology, unlike vicinal eliminations from neutral molecules (which pass through bona fide cyclic transition states). Cyclic topology is seen for a structure that precedes the potential energy maximum, but that ring disappears at the top of the barrier. Both syn elimination and ion−neutral complex formation from the radical cation proceed far along the pathway for bond heterolysis before arriving at a point at which the two types of mechanism diverge from one another.

Photochemically promoting an electron to the continuum (instead of to an unoccupied virtual orbital) does not fundamentally alter the physical processes that operate in isolated molecules. As in other areas of molecular photochemistry, the majority of reactions apparently take place from the lowest electronically excited state of appropriate multiplicity—in this case, the ground state doublet—regardless of the orbital from which an electron initially emerged. Photoions formed in the gas phase often fragment faster than they collide with other molecules, but vibrational energy tends to randomize internally prior to dissociation. Collections of molecules undergoing unimolecular decomposition in the absence of intermolecular collisions will not, in general, display single-exponential decay (since they contain a distribution of internal energies),[1] but a subset having a uniform internal energy will obey first-order kinetics.[2] In the latter instance the steady-state approximation proves useful in using first-order kinetic analyses for elucidating competing pathways.[3]

This paper examines deuterated analogues of the three simplest *sec*-alkyl phenyl ethers: 2-phenoxypropane (iPrOPh), 2-phenoxybutane (sBuOPh), and 3-phenoxypentane (3AmOPh). The abbreviations come from trivial names commonly applied to the respective alkyl groups: isopropyl, *sec*-butyl, and 3-amyl. It turns out that all three ethers have nearly the same adiabatic ionization energy. All of them give a single fragment ion upon low energy (<12 eV) photoionization: ionized phenol. However, that ostensible uniformity belies an underlying complexity of mechanism, which deuterium labeling reveals by means of the relative proportions of $PhOH^{\bullet+}$ and $PhOD^{\bullet+}$ observed as a function of internal energy. We find that no single mechanism accounts for the results. Branching ratios and isotope effects are extracted from the experimental data and interpreted with the aid of DFT calculations.

## Experimental Section

2-Phenoxy-*threo* and -*erythro*-3-$d_1$-butane and 2-phenoxy-2-$d_1$-butane were prepared as previously described.[4] $CH_3CH(OPh)CD_2CH_3$ was prepared by $Li_2CuCl_4$-catalyzed coupling[5]

† Dedicated to Bryan Kohler, in memory of his outstanding scientific accomplishments and the honor of his friendship.

10.1021/jp983886q CCC: $18.00 
Published on Web 02/23/1999

of $CH_3MgI$ with 2-phenoxy-1,1-$d_2$-*n*-propyl tosylate, while $CH_3CH(OPh)CH_2CD_3$ was prepared by $Li_2CuCl_4$-catalyzed coupling[5] of $CD_3MgI$ with 2-phenoxy-*n*-propyl tosylate. In similar fashion, $CH_3CH_2CH(OPh)CD_2CD_3$ was prepared by coupling $CD_3MgI$ with $CH_3CH_2CH(OPh)CD_2OTs$. $CD_3CH(OPh)CH_2CH_3$ was prepared by conversion of 2-phenoxybutyric acid to its methyl ester, reduction with $LiAlD_4$, conversion of the resulting alcohol to $CH_3CH_2CH(OPh)CD_2OTs$, and a second reduction with $LiAlD_4$. $CD_3CH(OPh)CD_2CH_3$ and $(CH_3CD_2)_2CHOPh$ were prepared by repetitive exchange of 2-butanone and 3-pentanone, respectively, with $D_2O$, followed by reduction with $LiAlH_4$, conversion to the tosylates, and displacement with sodium phenoxide in refluxing THF. $(CDH_2)_2CHOPh$ and $(CH_3CH_2)_2CDOPh$ were prepared by reduction of epibromohydrin and 3-pentanone, respectively, with $LiAlD_4$ followed by conversion to the tosylates and displacement with sodium phenoxide in refluxing THF. 2- and 3-Phenoxyoctane were prepared by conversion of the corresponding alcohols to their tosylates and displacement with sodium phenoxide in refluxing THF. All compounds were purified by at least two successive distillations and found to be free from chemical impurities (except for traces of volatile solvent) by GC/MS. Deuterium incorporation was found to be ≥98 atom % in all compounds except for $CD_3CH(OPh)CD_2CH_3$, which was 97 atom % D.

The apparatus for measuring photoionization efficiency (PIE) curves has been described in detail elsewhere.[3,6] Briefly, the microcomputer-controlled photoionization mass spectrometer makes use of the hydrogen pseudocontinuum and a Seya-Namioka monochromator equipped with a holographically ruled diffraction grating. The resolution of the monochromator was fixed at 1.35 Å, and the absolute energy scale was calibrated with atomic emission lines to an accuracy of better than 0.003 eV. All experiments were performed at ambient temperature (297 K) with sample pressures of $10^{-3}$ Pa in the ion-source region. Flight time between the ionization source and the mass selector is estimated to be on the order of 5 $\mu$s. Experimental adiabatic 0 K ionization energies (IEs) were measured for selected compounds and correspond to the first observed vibrational progression peak in the molecular ion first differential PIE curve. All first differential PIE curves were obtained from the experimental data using a 25-point Fourier transform filter for smoothing with the program HORIZON (Star Blue Software, Inc.) before simple first derivatives were taken. Experimental *m*/*z* 95:*m*/*z* 94 ratios were corrected for 6.6% natural abundance $^{13}C$ to obtain $PhOH^{\bullet+}$:$PhOD^{\bullet+}$ ratios, but no corrections were made for incomplete deuteration. Mechanistic models were fitted to the experimental ion ratios ($PhOH^{\bullet+}$:$PhOD^{\bullet+}$ or $PhOD^{\bullet+}$:$PhOH^{\bullet+}$, depending on which represented a value <1) using the MINSQ iterative nonlinear least-squares program in the SCIENTIST package (Micromath, Inc.). Branching ratios for each mechanistic model were determined at three wavelengths corresponding to extrema in the fragment ion intensity ratios in the first differential PIE curve. $Phenol^{\bullet+}$ was the only fragment ion observed at all energies, and its percent of the total ionization did not vary significantly among the *sec*-alkyl phenyl ethers, neither as a function of chain length nor as a function of deuteration: 15−30%Σ at 9.81 eV and 40−55%Σ at 10.36 eV; however, these ion abundances do differ signficantly from those measured for 1-phenoxypropane: 0.3−0.6%Σ at 9.81 eV and 10−12%Σ at 10.36 eV (again independent of deuteration).

Several mechanistic models were examined, of which three were were given special scrutiny. One model included the branching ratio for formation of ion−neutral complexes from ionized iPrOPh (*a*) and the isotope effect for proton transfer from an alkyl cation (*y*) among the adjustable parameters and assumed the primary isotope effects for $\beta$-elimination from a methyl (*u*) and from a methylene (*x*) to be equal. Another model was identical in all respects except that *a* was assumed to equal zero and *u* and *x* were allowed to vary independently. Neither of these models was able to give an exact fit to the 11.92 eV data. The preferred model, which gave exact solutions at all three photon energies, made use of the value of *y* previously reported from photoionization of 1-phenoxypropanes[3] and included *a*, *u*, and *x* among the independent parameters varied to fit the data. Estimated uncertainties in the derived branching ratios are based on ±5% uncertainties in the experimental $PhOH^{\bullet+}$:$PhOD^{\bullet+}$ ratios and were determined by Monte Carlo methods as follows. Using MATHEMATICA (Wolfram Research, Inc.), 1200 data sets were generated as random fluctuations (using a normal distribution with standard deviation of 5%) about the values from Figures 1−4 at a given photon energy, and best fit solutions found for each data set. Uncertainties are reported as the standard deviations among the derived values. Highly negatively correlated values (such as the 1- and

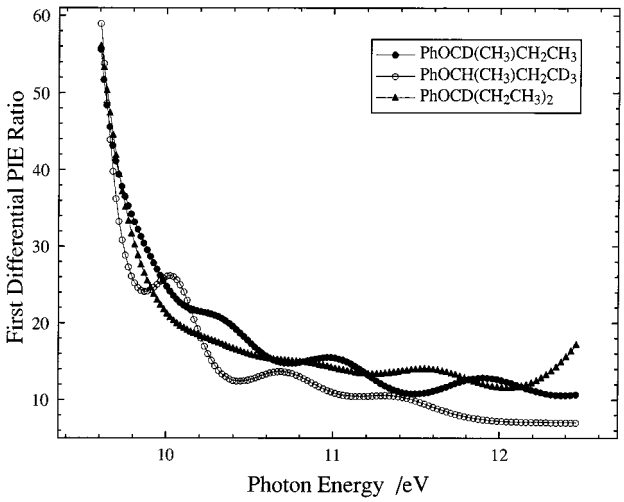


**Figure 1.** First differential $PhOH^{\bullet+}$:$PhOD^{\bullet+}$ photoionization efficiency ratios for 2-$d_1$-2-phenoxybutane (solid circles), 4,4,4-$d_3$-2-phenoxybutane (open circles), and 3-$d_1$-3-phenoxypentane (solid triangles).

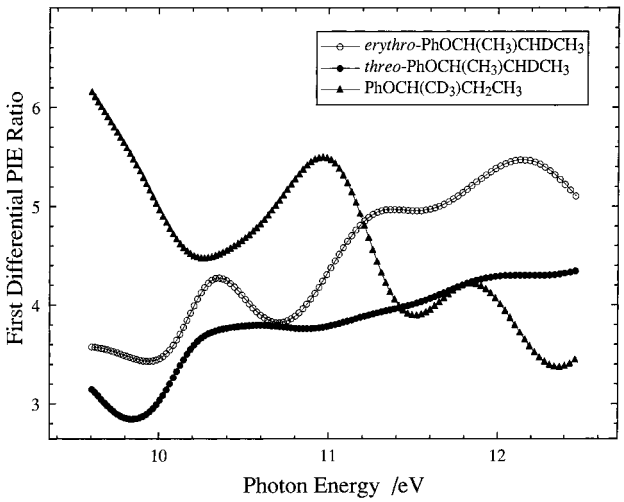


**Figure 2.** First differential $PhOH^{\bullet+}$:$PhOD^{\bullet+}$ photoionization efficiency ratios for *erythro*- (open circles) and *threo*-3-$d_1$-2-phenoxybutane (solid circles) and for 1,1,1-$d_3$-2-phenoxybutane (solid triangles).

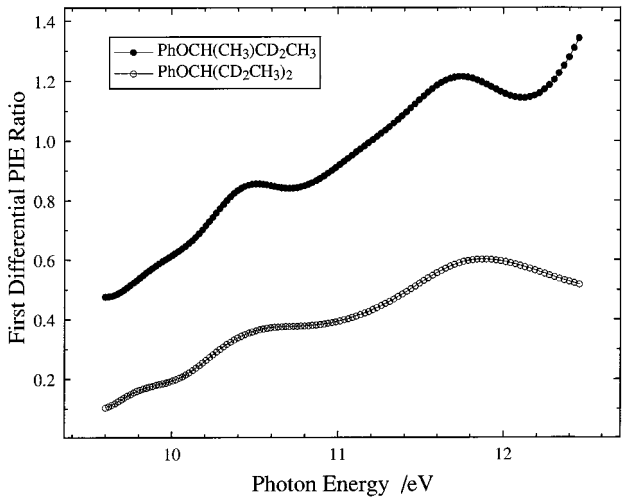


**Figure 3.** First differential $PhOH^{\bullet+}$:$PhOD^{\bullet+}$ photoionization efficiency ratios for 3,3-$d_2$-2-phenoxybutane (solid circles) and 2,2,4,4-$d_4$-3-phenoxypentane (open circles).

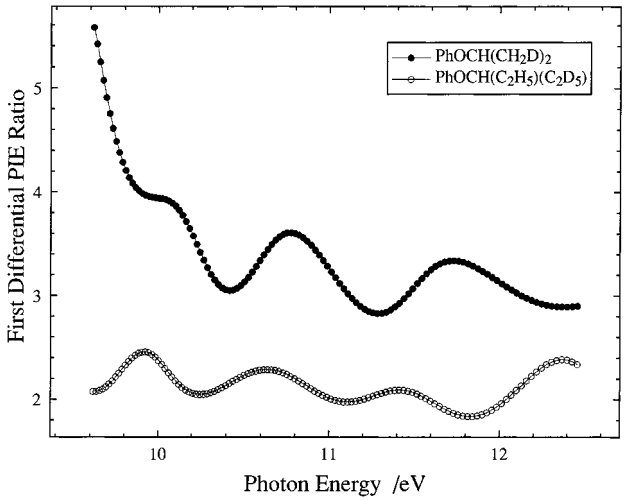


**Figure 4.** First differential $PhOH^{\bullet+}$:$PhOD^{\bullet+}$ photoionization efficiency ratios for 1,3-$d_2$-2-phenoxypropane (solid circles) and 1,1,1,2,2-$d_5$-3-phenoxypentane (open circles).

2-butenes from either decomposition pathway of ionized sBuOPh) have uncertainties symbolized by $\pm$ and $\mp$.

Ab initio calculations were performed with the 6-31G** basis set using the GAUSSIAN94 (Gaussian, Inc.) program system on a Cray T90 mainframe. Geometries were optimized using Hartree−Fock based and DFT (B3LYP) methods. DFT-optimized geometries and unscaled DFT zero-point energies were chosen for energetic estimates, since unrestricted Hartree−Fock based methods gave unacceptably high values of $\langle S^2 \rangle$.[7] Points along the $\beta$-elimination reaction path were calculated by performing DFT geometry optimizations with constrained O−CH distances. Bond paths and extrema of electron densities were evaluated using the PROAIMS suite of programs (from the AIMPAC program package kindly provided by J. Cheeseman and R. F. W. Bader). Theoretical estimates of $k_{CH_3}/k_{CD_3}$ for ionized $CH_3CH(CD_3)OPh$ were based on $3N-8$ DFT harmonic vibrational frequencies for each of the two transition states corresponding to alternative positioning of the methyl groups (with the internal rotation of the benzene ring about the phenoxy C−O axis treated as a free rotor), followed by direct counts of integrated densities of states to obtain the isotope effect as a function of internal energy. Use of the direct count algorithm became prohibitively expensive above 0.5 eV internal energy, so the theoretical estimate is compared with experiment only at $h\nu = 9.81$ eV.

**TABLE 1: Adiabatic Ionization Energies Measured for Selected *sec*-Alkyl Phenyl Ethers**

| compound | IE (eV) |
|---|---|
| *erythro*-$PhOCH(CH_3)CHDCH_3$ | 7.97 |
| $PhOCH(CD_3)CD_2CH_3$ | 7.98 |
| $PhOCH(CH_3)CH_2CD_3$ | 7.99 |
| 2-phenoxyoctane | 7.97 |
| $(CH_3CD_2)CHOPh$ | 7.94 |
| 3-phenoxyoctane | 7.93 |

## Results

Ionized alkyl phenyl ethers expel neutral alkenes to produce ionized phenol via two general decomposition pathways. One pathway, illustrated schematically in eq 1, proceeds via a pair of steps: heterolysis of a carbon−oxygen bond to form an ion−neutral complex (in which at least one of the partners can rotate independently of the other) followed by proton transfer from the cationic partner to the neutral phenoxy radical. As will be discussed below, intervention of ion−neutral complexes accounts for the formation of $PhOD^{\bullet+}$ from the $\alpha-$ and $\gamma$-deuterated analogues of sBuOPh, $PhOCD(CH_3)CH_2CH_3$ and $PhOCH(CH_3)CH_2CD_3$, as well as from the $\alpha$-deuterated analogue of 3AmOPh, $PhOCD(CH_2CH_3)_2$. As Figure 1 summarizes, $PhOD^{\bullet+}$ is virtually undetectable at the lowest ionizing energies studied but becomes steadily more abundant as the parent ion's internal energy increases.

$$ROPh^{\bullet+} \xrightarrow{\text{bond heterolysis}} [R^+ \quad PhO^{\bullet}] \xrightarrow{\text{proton transfer}} PhOH^{\bullet+} + \text{alkene} \quad (1)$$

The other pathway involves a 4-center elimination specifically from the $\beta$-positions (the hydrogens on the carbon adjacent to one to which oxygen is attached). This inference comes from the fact that the fragment ions have the structure of phenol (rather than one in which the itinerant hydrogen attaches to the ring)[8] and from the fact that (as Figure 2 depicts) the two diastereomers of $PhOCH(CH_3)CHDCH_3$ give different $PhOH^{\bullet+}$:$PhOD^{\bullet+}$ ratios. As has previously been argued,[4,8] eq 1 would not permit one to distinguish such stereoisomers mass spectrometrically.

**Photoionization Efficiency Measurements and Kinetic Analysis.** Table 1 summarizes adiabatic ionization energies (IEs) measured for selected *sec*-alkyl phenyl ethers. The IEs of the 2-phenoxyalkanes are found to be within experimental uncertainty ($\pm$0.02 eV) of the value we have previously reported for iPrOPh (7.98 eV).[3] The IEs for 3-phenoxyalkanes are slightly lower, 7.94 $\pm$ 0.02 eV. The position where phenoxy attaches to a *n*-alkane affects the IE, but deuteration and chain length apparently do not. The 298 K appearance energies for alkene expulsion, determined by threshold linear extrapolation, are 9.58 eV for iPrOPh, 9.39 eV for sBuOPh, and 9.34 eV for 3AmOPh ($\pm$0.03 eV). These values can be compared with the appearance energy for $PhOH^{\bullet+}$ from 1-phenoxypropane, 9.87 eV, for which we have previously published the PIE curve.[3]

Figures 1−4 plot the curves for deuterated analogues as ratios of the first differentials of $PhOH^{\bullet+}$ and $PhOD^{\bullet+}$ photoionization efficiencies (PIEs) in order to portray the effective product distributions as a function of internal energy of the molecular ion.[9] The energy spread of the parent ion at a given photon energy in a first differential plot is on the order of the thermal vibrational energy content of the parent neutral at 298 K, about

**SCHEME 1**

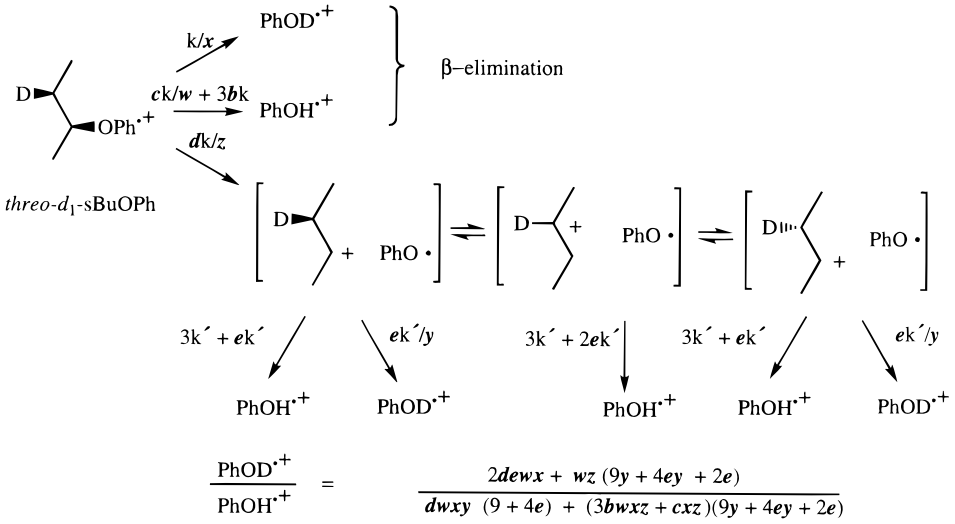


**SCHEME 2**

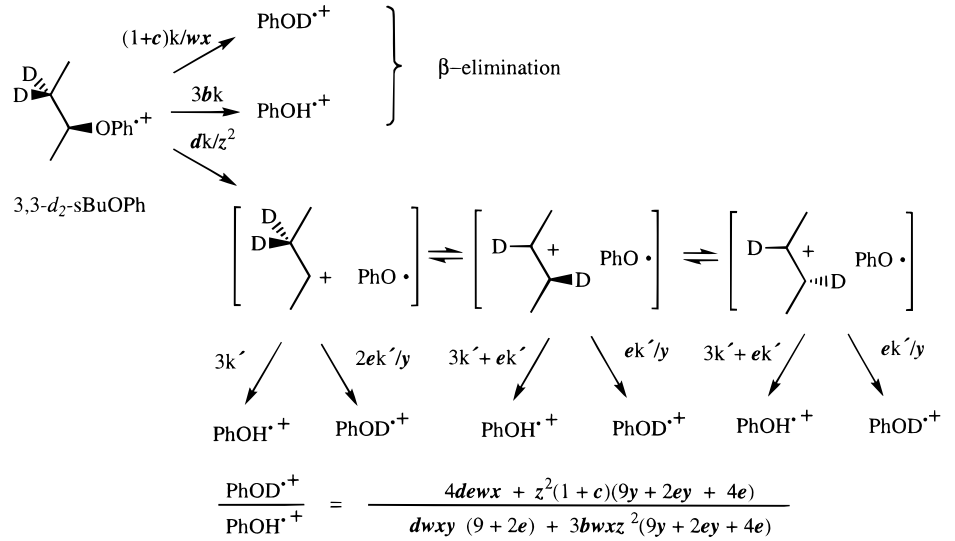


0.2 eV. Figure 1 shows results for compounds containing deuterium elsewhere than in the $\beta$-positions. Very little deuterium transfers in the fragmentations at the lowest ionizing energies. Figures 2 and 3 reproduce the ratios of the first differential PIE curves for compounds containing deuterium only in $\beta$-positions. The oscillations in Figure 2 appear somewhat exaggerated, owing to the scale chosen for the $y-$axis. Figure 3 exhibits results on a scale that gives a better idea of the magnitude of the oscillations (upon whose origin we do not speculate).

A straightforward interpretation of Figure 1 would suggest that the contribution from eq 1 increases with internal energy. At the lowest internal energies ($h\nu$ = 9.6 eV) ionization of 1,1,1,3,3-$d_5$-sBuOPh ($CD_3CH(OPh)CD_2CH_3$, curve not shown since it is virtually identical to the curve for $(CH_3CD_2)_2CHOPh$ in Figure 3) gives >8 times more $PhOD^{\bullet+}$ than $PhOH^{\bullet+}$, and we suspect that much of the $PhOH^{\bullet+}$ at this energy results from incomplete deuteration of the starting material. If we neglect ion−neutral complex formation at this internal energy (consistent with Figure 1), the results for the other $\beta$-deuterated analogues of sBuOPh imply that ionized sBuOPh eliminates 1-butene much less often than 2-butene and that the ratio of expelled *cis*-2-butene to *trans*-2-butene approximately equals the $PhOH^{\bullet+}$:$PhOD^{\bullet+}$ ratio for *threo* divided by the $PhOH^{\bullet+}$:$PhOD^{\bullet+}$ ratio for *erythro*. Mechanistic analysis provides a quantitative assessment of the relative contributions of competing pathways at higher internal energies. Schemes 1−3 illustrate first-order kinetics for decomposition of three deuterated analogues of ionized sBuOPh (one of the $d_1$, the $d_2$, and one of

**SCHEME 3**

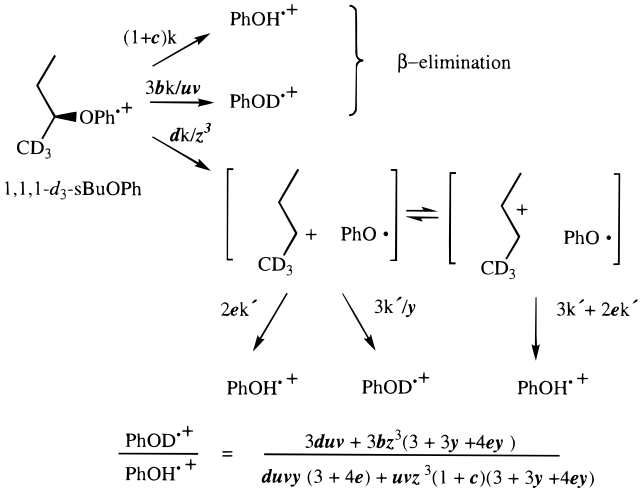

the $d_3$ isomers) by which branching ratios and isotope effects can be extracted from the experimental ratios.

The analysis of the fragment ion ratios for iPrOPh and sBuOPh employs 10 parameters chosen from among five branching ratios ($a-e$) and six independent $k_H/k_D$ values ($u-z$). Three models were examined and gave comparable branching ratios for sBuOPh. The first model ($a = 0$) supposes that ion−neutral complexes do not intervene at all in the decomposition of ionized iPrOPh (since previous studies have shown no evidence for exchange between the methyl and methine groups[10]). Three of the isotope effects were determined from the ratios measured for deuterated analogues of iPrOPh: $CH_3CH(OPh)CD_2H$ and $CD_3CH(OPh)CH_3$, for which we have previously published PIE ratios, and $(CDH_2)_2CHOPh$, whose first differential PIE curve is reproduced in Figure 4. The ratio for this last compound depends on two consequences of deuterium substitution, a primary ($u$) and a secondary isotope effect ($w$) affecting $\beta$-elimination.

$$\frac{\mathrm{PhOD}^{\bullet+}}{\mathrm{PhOH}^{\bullet+}} = \frac{1/u}{2/w} = \frac{w}{2u} \tag{2}$$

We then take the ratio for the other $d_2$-analogue, $CH_3CH(OPh)CD_2H$, to depend on the combination of those two isotope effects as well as a third one, the secondary isotope effect resulting from having two deuteria attached to the same methyl group ($v$). The primary ($u$) times the secondary ($w$) isotope effect gives the net $k_H/k_D$ for transfer of deuterium from the $CHD_2$ group. The ratio for $CH_3CH(OPh)CD_2H$ thus equals

$$\frac{\mathrm{PhOD}^{\bullet+}}{\mathrm{PhOH}^{\bullet+}} = \frac{2/uw}{(1/v) + 3} = \frac{2v}{uw + 3uvw} \tag{3}$$

Finally, the deuterium isotope effect for transfer from a $CD_3$ versus a $CH_3$ results from the combined primary isotope effect $u$ and the secondary isotope effect $v$, giving

$$\frac{\mathrm{PhOD}^{\bullet+}}{\mathrm{PhOH}^{\bullet+}} = \frac{3/uv}{3} = \frac{1}{uv} \tag{4}$$

The second model ($y$-fixed) takes the isotope effect $y$ for the acid−base reaction within an ion−neutral complex (the second step of eq 1) to have the same value, $y = 1.21 \pm 0.03$, as we have reported for [$iPr^+$ $PhO^{\bullet}$] complexes from ionized 1-phenoxypropenes.[3] For the higher homologues of iPrOPh, parameter $y$ represents a composite effect, based on the assumption that the isomeric *sec*-butyl cations from a given precursor (such as those drawn within the ion−neutral complexes in Schemes 1−3) all contribute equally. Similarly, the use of this single parameter for *sec*-pentyl cations supposes that isotopic label distributes itself randomly among the middle three carbons.

Since $y$ is not a variable in the $y$-fixed model, we can solve for a parameter not included in the $a = 0$ model, namely the branching ratio ($a$) for decomposition of ionized iPrOPh via [$iPr^+$ $PhO^{\bullet}$] ion−neutral complexes. Instead of using eqs 2−4 to extract isotope effects $u$, $v$, and $w$, the $y$-fixed model derives more complex expressions, as illustrated in Scheme 4 for for 1,1,1-$d_3$-2-phenoxypropane. The three new expressions for deuterated iPrOPh were combined with those from sBuOPh (identical to those used in the $a = 0$ model, except that a constant is subsituted for $y$) and solved for the branching ratios $a-e$ and the isotope effects $u-x$ and $z$. In both models, parameter $z$ symbolizes the average $\beta$-secondary isotope effect on bond heterolysis (the first step of eq 1) and is assumed to be multiplicative (such that, for example, the three $\beta$-deuteria in

**SCHEME 4**

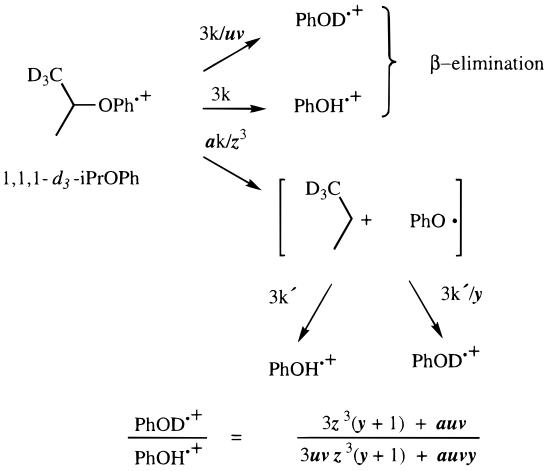


**TABLE 2: Fraction of Decomposition of Undeuterated *sec*-Alkyl Phenyl Ether Radical Cations Taking Place via Ion−Neutral Complexes, Determined from Ratios of First Differential PIEs (Uncertainties Given Only for the *y*-Fixed Model) for Various Mechanistic Models[a]**

| | | ion internal energy | | |
|---|---|---|---|---|
| ion | model | 1.9 eV | 2.4 eV | 4.0 eV |
| $iPrOPh^{\bullet+}$ | $u = x$ | 0.65 | 0.64 | *b* |
| | $y = 1.21$ | 0.52 ± 0.12 | 0.62 ± 0.10 | 0.60 ± 0.05 |
| | $y = 1.0$ | 0.41 ± 0.16 | 0.56 ± 0.09 | 0.55 ± 0.05 |
| $sBuOPh^{\bullet+}$ | $a = 0$ | 0.13 | 0.22 | *b* |
| | $u = x$ | 0.33 | 0.30 | *b* |
| | $y = 1.21$ | 0.191 ± 0.011 | 0.326 ± 0.020 | 0.518 ± 0.025 |
| | $y = 1.0$ | 0.159 ± .014 | 0.279 ± .016 | 0.451 ± 0.017 |
| $3AmOPh^{\bullet+}$ | $a = 0$ | 0.13 | 0.32 | *b* |
| | $u = x$ | 0.34 | 0.36 | *b* |
| | $y = 1-1.4$ | 0.188 ± 0.017 | 0.384 ± 0.039 | 0.557 ± 0.064 |

[a] Internal energies correspond to the three photon energies at which data analyses were performed (9.81, 10.36, and 11.92 eV). the $a = 0$ model assumed the fraction to be zero for ionized iPrOPh. [b] No solution found to fit the data.

Schemes 3 and 4 attenuate formation of ion−neutral complexes by a factor of $z^3$ relative to their undeuterated analogues). Since secondary isotope effects do not necessarily act cumulatively, this assumption may lead to systematic error.

The third model supposes that the same primary isotope effect operates for a monodeuterated methyl group ($CH_2D$) as for a monodeuterated methylene (CHD), i.e., $u = x$. In two of the models the fraction of ionized sBuOPh decomposing via complexes increases with internal energy, as Table 2 summarizes, but in the $u = x$ model that fraction does not change significantly between 9.81 and 10.36 eV. Neither the $a = 0$ model nor the $u = x$ model succeeds in fitting the 11.92 eV first differential ratios, but the $y$-fixed model does. Hence we believe the $y$-fixed model to give the most credible results and report the branching ratios determined using $y = 1.21$ in Scheme 5. In part this choice is justified by our finding that a ±10% variation in $y$ contributes no more to the uncertainty of the derived values than does a 5% uncertainty in the experimental ratios. As Table 2 shows, neglecting this isotope effect altogether (i.e., $y = 1.0$) has a comparatively small effect on the contribution of ion−neutral complexes inferred from the experimental data.

The branching ratios derived using the $y$-fixed model ($y = 1.21$) for sBuOPh are tabulated in Scheme 5 and those for 3AmOPh in Scheme 6. The latter are based on results (plotted in Figures 1, 3, and 4) for 3-$d_1$, 2,2,4,4-$d_4$, and 1,1,1,2,2-$d_5$ analogues of 3AmOPh, in which the isotope effect on $\beta$-elim-

**SCHEME 5**

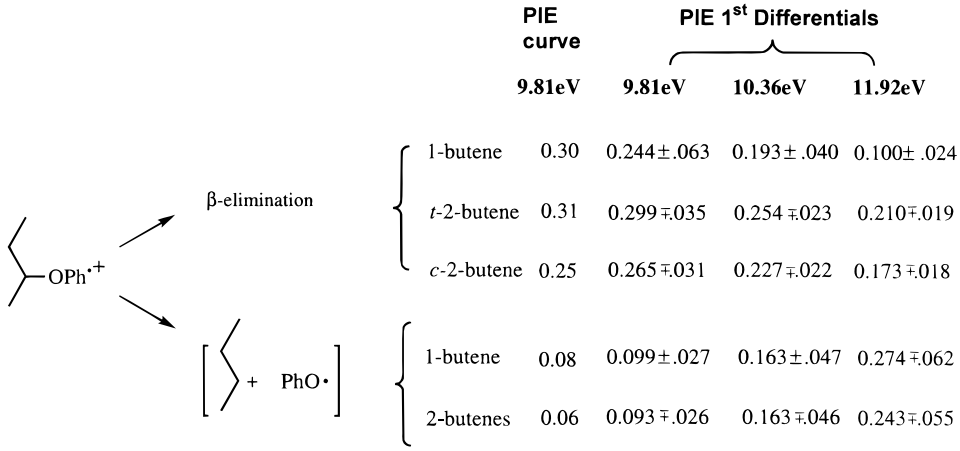


**SCHEME 6**

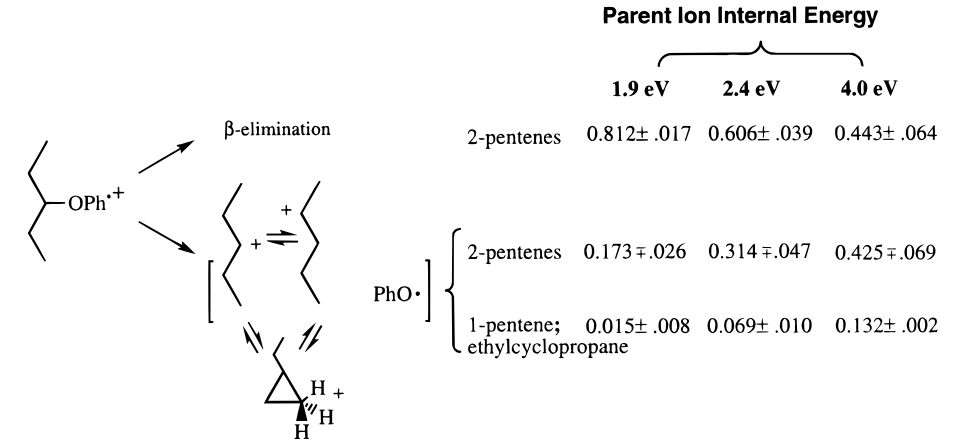


**TABLE 3: Kinetic Isotope Effects for *β*-Elimination of Deuterium versus Hydrogen Derived from Steady State Analyses of the Lowest Energy PIE Data (Ratios of Ion Abundances) and of the Experimental First Differential PIE Curves of 10 Deuterated Analogues of iPrOPh and sBuOPh based on the *y*-fixed model**

| | | PIE[a] | | internal energy for first differentials[b] | | |
|---|---|---|---|---|---|---|
| symbol | definition | 9.6 eV | 9.8 eV | 1.9 eV | 2.4 eV | 4.0 eV |
| *u* | primary isotope effect for iPrOPh | 1.41 | 1.80 | 1.80 ± 1.08 | 1.76 ± 0.91 | 1.69 ± 0.49 |
| *uv* | $k_{CH_3}/k_{CD_3}$ for a methyl group | 1.56 | 5.32 | 3.18 ± 1.76 | 2.27 ± 0.91 | 1.80 ± 0.36 |
| *x* | methylene primary $k_{CH_2}/k_{CHD}$ in sBuOPh | 2.33 | 1.10 | 1.24 ± 0.24 | 1.52 ± 0.21 | 1.46 ± 0.14 |
| *wx* | $k_{CH_2}/k_{CD_2}$ for sBuOPh methylene | 2.10 | 0.71 | 0.88 ± 0.27 | 1.09 ± 0.23 | 0.72 ± 0.12 |

[a] From ratios of ion abundances in the photoionization efficiency curves. [b] From ratios of the first differential PIE curves.

ination from a $CD_2$ group (symbolized as *t*) is not assumed to be the same as for sBuOPh. The *β*-deuterium isotope effects on ion−neutral complexes, *z* (per *β*-deuterium), are taken to be the same as for the lower homologues: 0.91 ± 0.03 at 9.81 eV, 0.94 ± 0.03 at 10.36 eV, and 0.86 ± 0.03 at 11.92 eV. The uncertainties in Scheme 6 (and for isotope effect *t*, which has a value of 2.5 at all internal energies, but whose uncertainty ranges for ±0.2 at 1.9 eV to ±0.6 at 2.4 eV to ±1.8 at 4.0 eV) reflect the variation in derived branching ratios resulting from allowing *y* to take on values from 1.0 to 1.4.

Table 3 summarizes the deuterium isotope effects for *β*-elimination derived using the *y*-fixed model. Large uncertainties in the $k_H/k_D$ values accompany the comparatively small uncertainties in branching ratios. The supposition that deuterium in the *γ*-position of ionized 3AmOPh does not affect its rate of heterolysis is open to question, since computation indicates that corner-protonated ethylcyclopropane (drawn in equilibrium with the secondary cations in the ion−neutral complex at the bottom of Scheme 6) has the same stability as the classical 3-pentyl cation and interconverts easily with it.[11] Therefore, the difference between $k_{CH_2}/k_{CD_2}$ for a 3AmOPh methylene (*t*) and for a sBuOPh methylene (*wx*), though statistically significant, may reflect systematic errors introduced by the necessity of using single parameters, *y* and *z*, to characterize the consequences of deuteration on the rates of creating and destroying ion−neutral complexes. Given the magnitude of the experimental uncertainties, there is no evidence that any of the isotope effects changes significantly as a function of internal energy.

As Scheme 5 summarizes, the branching ratios for sBuOPh derived at $h\nu = 9.81$ eV are nearly the same, regardless of whether one uses the ratio of experimental ion abundances (where the least-squares program does not find an exact fit) or their first derivatives. This instills confidence in our use of first differential values at higher photon energies. As Table 3 summarizes, the isotope effects from the PIE ratios display some peculiarities, though they do not differ significantly from the values derived from first differentials. Since the 9.8 eV PIE ratios represent a superposition of ions with various internal

energies, they must be considered less reliable. The data at energies below 9.8 eV (whether PIE ratios or first differentials) cannot be fit, even if one assumes no formation of ion−neutral complexes whatsoever and takes the ratios in Figure 1 all to be zero (as well as the $PhOH^{\bullet+}$:$PhOD^{\bullet+}$ ratio from $CD_3CH(OPh)$-$CD_2CH_3$).

**Theoretical Calculations.** sBuOPh has five chemically distinct types of $sp^3$ CH bonds: the methyl near the oxygen (position 1), the methyl further from the oxygen (position 4), the hydrogen attached to the same carbon as the oxygen (the α-hydrogen, position 2), and the stereochemically differentiable methylene hydrogens (*erythro* and *threo* at position 3). Formerly, it was thought that substituting each of these individually would permit an unambiguous assessment of the positional and stereochemical selectivity of a reaction in terms of the fractional contribution from each site. Recently, however, we pointed out that such a phenomenological interpretation can lead to contradictions and that a mechanistic analysis is to be preferred, even though it requires the study of additional isotopically substituted analogues.[3] Given a set of mechanistic hypotheses, the relative product yields from a unimolecular decomposition can be dissected using a first-order kinetic scheme (either by solving a set of coupled differential equations[12] or by means of the steady-state approximation[3]) under the following circumstances: the concentration of the reactant must decay exponentially (as when it rapidly equilibrates with an infinite heat bath or consists of a set of isolated, monoenergetic molecules[2]) or else the reaction must have gone to completion (in which case the result represents an ensemble average). While there are other circumstances where a steady-state analysis provides a satisfactory approximation,[13] the photoionization results analyzed above correspond to collections of essentially monoenergetic reactants.

Our analysis of ionized sBuOPh discerns two mechanisms: β-elimination (in which hydrogen transfers specifically from positions 1 and 3 and which can differentiate erythro from threo) and complex formation (in which the itinerant hydrogen can originate from any of the alkyl positions and where stereochemical distinctions are lost). One can conceive alternative mechanistic options, but those two pathways have precedents and suffice to account for the data in hand.


**1**


**2**

Theoretical calculations probe what experiment cannot yet ascertain definitively: whether β-elimination might be proceeding via ion−neutral complexes, in which the alkyl cations remain fixed in their most stable geometries. The two lowest energy computed structures for *sec*-butyl cation, **1** and **2**, have bridging atoms.[14] The accessibility of **1**, with a bridging proton, explains the low-barrier interconversions of classical structures represented in Schemes 1-3 (for which condensed phase studies show ample precedent[15]). On the one hand, it is apparent that ion−neutral complexes containing **1** cannot account for β-elimination, since the two methyl groups are equivalent in this ion. Experimentally, β-elimination from ionized sBuOPh excludes one methyl (position 4) even as it includes the other (position 1). On the other hand, **2** (which has a bridging methyl and corresponds to a corner-protonated cyclopropane) preserves the distinction among the five types of hydrogen and renders only the *erythro* and *threo* hydrogens (one being cis and the other trans to the α-hydrogen) and the nonbridging methyl acidic enough to transfer a proton to form alkenes. A [**2** $PhO^{\bullet}$] complex would display all the characteristics so far observed experimentally for β-elimination.

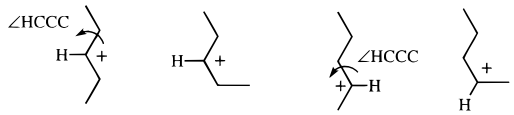


**3** **4** **5** **6**

**TABLE 4: Calculated Electronic Energies and Dihedral Angles (B3LYP/6-31G**) for Isomeric *sec*-Pentyl Cations**

| ion | isomer | $E_{el}$ (au) | ∠HCCC (deg) |
|---|---|---|---|
| **3** | *trans*,*trans*-3-pentyl | −196.865 950 | 31 |
| **4** | *cis*,*trans*-3-pentyl | −196.864 567 | 41, 162 |
| **5** | *trans*,*trans*-2-pentyl | −196.863 674 | 38 |
| **6** | *cis*,*trans*-2-pentyl | −196.862 372 | 162 |

Similarly, complexes containing noninterconverting cations could conceivably lead to exclusive β-elimination from ionized 3AmOPh. Density functional (DFT) geometry optimizations using the B3LYP approach[16] show the all-trans structure **3** (which has $C_2$ symmetry, even though that was not imposed as a constraint) to be the most stable classical secondary pentyl cation, as Table 4 summarizes. Were the classical 3-pentyl cations, **3** and its rotamer **4**, the only cations in ion−neutral complexes, exclusive β-elimination would be observed. Interconversion with corner-protonated cyclopropanes (such as illustrated at the bottom of Scheme 6) would not necessarily affect this. Isomerization to 2-pentyl cations (**5** or **6**) would have to have taken place for the α-hydrogen to transfer to oxygen.

The same arguments apply to ionized iPrOPh, since there is no evidence for transposition of hydrogens at any energy.[10] Our distinction between the two most plausible ways to analyze the experimental data, the *y*-fixed and $a = 0$ models, hinges on whether β-elimination from $iPrOPh^{\bullet+}$ occurs without the intervention of complexes. On the basis of the *y*-fixed model, we conclude that about half the decomposing ions pass through [$iPr^+$ $PhO^{\bullet}$] complexes when the parent ion contains 1.85 eV internal energy. If, on the other hand, all dissociations of $iPrOPh^{\bullet+}$ take place via a single mechanism, the *y*-fixed model does not pertain. Our surmise that complexes intervene less and less at lower energies has been tested by DFT calculations on the consequences of elongating the $sp^3$ C−O bond of ionized iPrOPh. Table 5 summarizes the outcome. Basis set superposition error (BSSE) was estimated using counterpoise for the noncovalently bound structures in which the partners (phenoxy radical and isopropyl cation or ionized phenol and propene) have nearly the same structures as their free counterparts.[17]

A four-member transition state is found for β-elimination, structure **A** drawn in Figure 5, for which a DFT normal modes calculation shows one negative force constant. The energy of this transition state relative to ionized iPrOPh (the radical cation), 1.15 eV (when unscaled zero-point energies are taken into consideration), is consistent with the experimental value <1.33 eV.[7] The geometry of the transition state corresponds to syn elimination, which is our reason for correlating the expulsion of *trans*-2-butene with formation of $PhOD^{\bullet+}$ from the *threo* precursor and the expulsion of neutral *cis*-2-butene with formation of $PhOD^{\bullet+}$ from the *erythro*. Structure **A** in Figure 5 will be denoted as the syn transition state.

In contrast to this transition state we find the ion−neutral complex to have a higher energy. Ion−neutral complexes need not correspond to minima on the potential energy surface. Their hallmark is that one of the partners (the isopropyl cation, in this case) must rotate about an axis orthogonal to the bond that

**TABLE 5: Calculated Electronic Energies (in atomic units), Net Electronic Spin, and Geometrical Parameters (B3LYP/6-31G**) for Ionized iPrOPh in Its Most Stable Geometry (the Radical Cation), in Its Constrained ($r_{OC}$ = 2.6 Å) Geometry, for the $\beta$-Elimination (syn) Transition State, for the $C_2$ Symmetry Constrained Ion−Neutral Complex, for the Aggregate of Propene with Ionized Phenol, and for Phenoxy Radical plus Isopropyl Cation[a]**

| | radical cation | constrained | transition state | [iPr$^+$PhO$^\bullet$] | propene···HOPh$^{\bullet+}$ | PhO$^\bullet$ and iPr$^+$ |
|---|---|---|---|---|---|---|
| $-E_{el}$ (au) | 425.147118 | 425.099275 | 425.097805 | 425.089099 | 425.122060 | 425.057871 |
| $\langle S^2\rangle$ | 0.7672 | 0.7806 | 0.7783 | 0.7809 | 0.7666 | 0.7898 |
| ZPE (eV)[b] | 5.143 | *d* | 4.949[e] | 4.926[e] | 5.046 | 4.869 |
| distances (Å) | | | | | | |
| $r_{OC}$ | 1.498 | 2.600 | 2.688 | 2.897 | 3.093 | ∞ |
| $r_{OH}$ | 2.64[c] | 2.180 | 1.748 | 3.701 | 1.012 | ∞ |
| $r_{CC}$ | 1.518 | 1.448 | 1.416 | 1.446 | 1.346 | 1.441 |
| $r_{CH}$ | 1.09[c] | 1.114 | 1.163 | 1.097 | 2.005 | 1.117 |
| $r_{CMe}$ | 1.522 | 1.456 | 1.460 | 1.446 | 1.497 | 1.441 |
| $r_{SC\alpha H\alpha}$ | 1.093 | 1.089 | 1.091 | 1.101 | 1.091 | 1.094 |
| $r_{sp^2-CO}$ | 1.305 | 1.268 | 1.270 | 1.263 | 1.302 | 1.258 |
| angles (deg) | | | | | | |
| $\angle C_\beta C_\alpha Me$ | 114.6 | 124.2 | 125.4 | 124.8 | 125.6 | 126.1 |
| $\angle OC_\alpha C_\beta$ | 104.9 | 87.6 | 78.7 | 117.6 | 73.9 | |
| $\angle OH_\beta C_\beta$ | 65[c] | 121.7 | 145.0 | 86.2 | 172.5 | |
| $\angle H_\beta C_\beta C_\alpha$ | 111[c] | 102.1 | 92.3 | 111.9 | 79.7 | 102.8 |
| $\angle H_\beta OC_\alpha$ | 55[c] | 48.7 | 43.7 | 37.8 | 23.9 | |
| $\angle H_\alpha C_\alpha Me$ | 111.8 | 117.9 | 117.0 | 117.6 | 116.1 | 117.0 |
| $\angle H_\alpha C_\alpha O$ | 106.8 | 83.2 | 85.7 | 0 | 101.7 | |
| $\angle sp^2$-$COC_\alpha$ | 125.0 | 144.1 | 170.1 | 180 | 138.5 | |
| dihedral angles and angles of bonds with planes (deg) | | | | | | |
| $\angle OC_\alpha C_\beta H_\beta$ | ±61[c] | 0.4 | 3.0 | 37.5 | 2.4 | |
| $\angle sp^2$-$COC_\alpha C_\beta$ | 151.0 | 170.3 | 167.7 | 0 | −36.1 | |
| $\eta$ | 54[c] | 43.4 | 33.3 | 54.7 | 7.5 | 60.6 |
| $\zeta$ | 46.6 | 4.4 | 2.1 | 0 | 1.0 | 0 |
| $\tau$ | 28.2 | 8.8 | 5.6 | 61.7 | 28.5 | |
| $\psi$ | 8.2 | 51.6 | 79.3 | 0 | 34.4 | |

[a] Symbols for geometrical parameters are defined in Figure 5. [b] Zero-point energy from unscaled B3LYP/6-31G** normal mode. [c] Mean of the values for two different choices for $H_\beta$. [d] Not an extremum, normal modes not calculated. [e] One negative force constant.

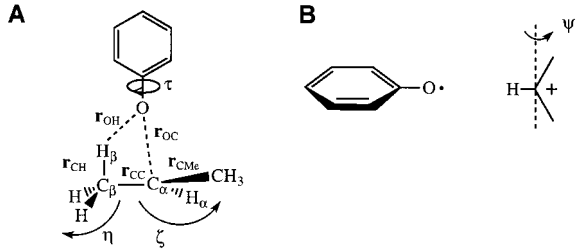


**Figure 5.** Optimized geometries (B3LYP/6-31G**) of (**A**) the syn transition transition state for $\beta$-elimination and (**B**) the $C_2$-constrained ion−neutral complex from ionized iPrOPh.

has severed.[18] Therefore, we chose structure **B** drawn in Figure 5 (constrained to have $C_2$ symmetry) to represent the ion−neutral complex, and we calculate its energy to be 1.37 eV above that of the iPrOPh$^{\bullet+}$ radical cation. This is slightly greater than the experimental upper bound measured for the barrier to propene elimination.[7] With a counterpoise correction for BSSE the electronic energy of **B** lies 0.80 eV below the electronic energy calculated for free isopropyl cation and phenoxy radical.

Figure 6 summarizes the energies of the relevant extrema along the reaction coordinate for elimination of propene from the iPrOPh$^{\bullet+}$ radical cation, taking into consideration the unscaled DFT zero-point energies. **A** and **B** both exhibit one negative force constant, while the other structures display only positive force constants. Subsequent to hydrogen transfer, the potential energy drops to a local minimum corresponding to a cluster of propene with ionized phenol, propene···HOPh$^{\bullet+}$. With a counterpoise correction for BSSE, the electronic energy for this aggregate lies 0.53 eV below that of the separated products, but we have no experimental evidence for its intermediacy. The potential well for propene···HOPh$^{\bullet+}$ is shallower than the one

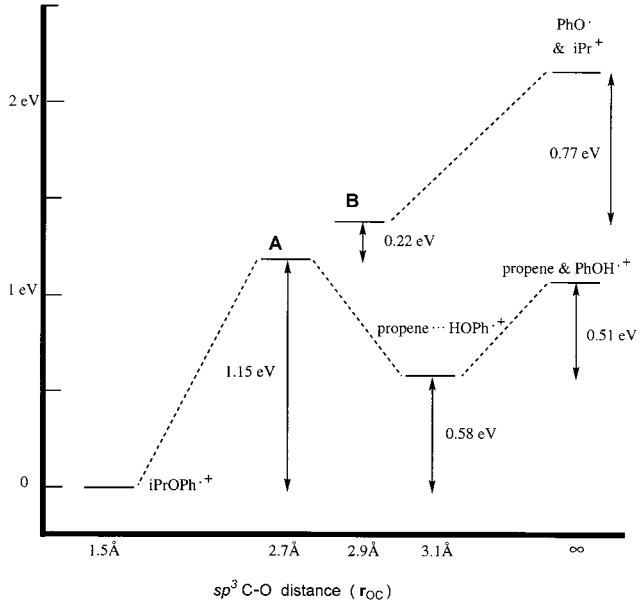


**Figure 6.** DFT energies (including unscaled ZPE corrections) relative to ionized isopropyl phenyl ether (iPrOPh$^{\bullet+}$) for extrema along the competing decomposition pathways, including transition structures **A** and **B** in Figure 5.

for **B**, which exemplifies the importance of the polarizability and dipole moment of the uncharged partner in stabilizing the interactions between ions and neutrals. The calculated energy of the separated products relative to iPrOPh$^{\bullet+}$, 1.10 eV, does not differ greatly from the experimental value, 1.05 eV.[7]

Along the reaction coordinate, a geometry optimized with the sp$^3$ C−O bond length ($r_{OC}$) constrained to be 0.088 Å shorter than that of the syn transition state has an electronic energy

1.30 eV above that of the iPrOPh$^{\bullet+}$ radical cation. Figure 6 does not include this constrained structure, because it does not correspond to a local minimum or saddle point. Between the constrained structure and transition state **A** several major geometric changes take place: the O−H distance ($r_{OH}$) shortens by 0.43 Å and the CH$_\beta$ bond ($r_{CH}$) elongates by 0.05 Å, along with the attendant changes in bond angles summarized in Table 5. Torsion angle $\tau$ stands for the angle made by the C$_\alpha$−C$_\beta$ bond with the plane of the ring. Some bond lengths do not vary monotonically in passing from ionized iPrOPh to the syn transition state. The bond from the central carbon of the isopropyl to the nonreactive methyl ($r_{CMe}$) and the bond from the benzene ring to oxygen ($r_{sp^2-CO}$) both become shorter in the constrained structure than in either the transition state or the radical cation. These bond shrinkages are what would be expected for an incipient heterolysis, where subsequent transfer of H$_\beta$ circumvents formation of an ion−neutral complex as the sp$^3$ C−O gets longer. An atoms-in-molecules analysis of extrema in the electron density provides additional insight, as the discussion below will present.

## Discussion

Ionized *sec*-alkyl phenyl ethers expel neutral alkenes via two competing unimolecular pathways in the gas phase, as revealed by isotopic labeling studies. One pathway, $\beta$-elimination, manifests a moderate degree of stereospecificity, which has rendered it useful for mass spectrometric analysis of other stereospecific reactions.[19] The work presented here examines the energetic dependence of this pathway relative to the formation of [*sec*-alkyl cation PhO$^\bullet$] complexes. The three simplest examples correspond to molecules in which the central carbon is flanked by two methyls, iPrOPh = MeCH(OPh)Me; a methyl and an ethyl, sBuOPh = MeCH(OPh)Et; and two ethyls, 3AmOPh = EtCH(OPh)Et. Assumptions about the transferability of isotope effects among these three leads to experimental determinations of branching ratios, as tabulated above in Schemes 5 and 6.

The choice of mechanistic model determines the outcome of the data analysis. This choice hinges on whether ionized iPrOPh decomposes by a single pathway or via competing mechanisms. A plausible theoretical picture has been computed for iPrOPh$^{\bullet+}$, which will be discussed below in greater detail. It portrays two competing mechanisms separated in energy by approximately 0.2 eV. The relative proportions of $\beta$-elimination (relative to formation of ion−neutral complexes) ought to decrease as energy content increases until a plateau is reached, consistent with our interpretation of the experimental data (cf. Table 2). For ionized sBuOPh and 3AmOPh, kinetic analysis shows that approximately 20% of parent ions with 1.9 eV internal energy dissociate via ion−neutral complexes. With 2.4 eV internal energy 30−40% of the decomposing ions pass through complexes. With 4.0 eV the fraction is 50−60%.

The present results for ion−neutral complexes can be compared with data from neutral product studies of gaseous ions. Ionized 1-phenoxybutane decomposes via [*sec*-Bu$^+$ PhO$^\bullet$] ion−neutral complexes,[20] and the expelled alkenes have been examined by EBFlow analysis.[21] The reported distribution of deuterium in the 2-butenes recovered from PhOCH$_2$CD$_2$CH$_2$CH$_3$ is consistent with complete scrambling of 1 hydrogen with 2 deuteria,[20−22] as Scheme 2 depicts for a different starting material. Very little methylcyclopropane is recovered from ionization of 1-phenoxybutane, and the ratio of 1-butene to 2-butenes among the EBFlow products is close to unity, in excellent agreement with the proportions from [*sec*-Bu$^+$ PhO$^\bullet$] inferred on the basis of the photoionization experiments summarized in Scheme 5. Ions within these complexes do not undergo any carbon skeleton rearrangement, as free ions do.[24] The cis/trans ratio from the complex cannot be deduced from the photoionization results, but ionized PhOCH$_2$CH$_2$CH$_2$CH$_3$ yields a 50:50 mixture in the recovered neutral products. This contrasts with the behavior of free C$_4$H$_9^+$ in the EBFlow, where deprotonation with dimethyl ether (whose gas phase basicity is comparable to that of a phenoxy radical) gives an isomer ratio of 0.3 and yields even more methylcyclopropane than *cis*-2-butene.[23] Free C$_4$H$_9^+$ ions behave as one would expect based on ab initio calculations, which show the proton-bridged structure **1** with *trans*-methyls and the corner-protonated cyclopropane **2** to be the most stable isomers of the *sec*-butyl cation.[14] The C$_4$H$_9^+$ within ion−neutral complexes, however, behaves like the interconverting classical cation structures drawn in Schemes 1−3.

Our analysis of the photoionization experiments dissects $\beta$-elimination away from the component that proceeds via eq 1 and permits a quantitative determination of the stereospecificity of the former. The branching ratio *c* (the ratio of *erythro* versus *threo* hydrogen transfer for sBuOPh) translates directly into cis/trans ratio of 2-butene expelled by $\beta$-elimination. This ratio does not depend on which of the three mechanistic models is used to extract it from the data, and it does not vary significantly with internal energy: $c = 0.89 \pm 0.05$, $0.90 \pm 0.05$, and $0.83 \pm 0.06$ at the three photon energies studied (not far from the ratio of PhOD$^{\bullet+}$:PhOH$^{\bullet+}$ ratios from the *erythro*- and *threo*-$d_1$ isomers at those energies). We infer that the net preference for expulsion of *trans*-alkene via $\beta$-elimination does not change very much over the energy domain from onset to 4 eV internal energy.

We have computed the isotope effect $k_{CH_3}/k_{CD_3}$ for $\beta$-elimination from ionized CH$_3$CH(OPh)CD$_3$ (based on normal modes calculations for the syn transition state). The experimental $k_{CH_3}/k_{CD_3}$ values (Table 3) have such large uncertainties that no meaningful comparison can be made with the theoretical rate of transfer from the CH$_3$ relative to the CD$_3$. We predict $k_{CH_3}/k_{CD_3} = 1.47$ for the syn transition state at an internal energy of 0.5 eV (the internal energy corresponding to 9.81 eV minus the experimental upper bound for the barrier height), a value that looks plausible and lies within one standard deviation of the experimental value of $u\nu$ based on the *y*-fixed model. The 9.81 eV values of $k_{CH_3}/k_{CD_3}$ from the $a = 0$ model (1.49) and from the $u = x$ model (1.36) also do not differ significantly from the theoretical prediction.

**Atoms-in-Molecules Analysis.** Now consider the extrema of the electron density $\rho$ within the syn transition state.[25] Two types of saddle points in $\rho$ are found for iPrOPh$^{\bullet+}$: bond critical points (one positive and two negative second derivatives), which occur between bonded atoms, and ring points (one negative and two positive second derivatives) which correlate with cyclic topologies. Ring points are found inside the benzene ring (coplanar with the 6 sp$^2$ carbons) but nowhere else in the radical cation or in the syn transition state (represented by structure **A** in Figure 5). That is to say, theory shows no evidence that the syn transition state contains a second ring. The constrained structure with $r_{OC} = 2.6$ Å does have cyclic topology, with bond critical points between C$_\alpha$ and oxygen and between H$_\beta$ and oxygen (as well as a second ring point), but the former has disappeared by the time the top of the barrier is reached. The atoms-in-molecules picture of $\beta$-elimination can be summarized as follows. The isopropyl−oxygen bond in ionized iPrOPh stretches until the alkyl group begins to resemble an alkyl cation,

**TABLE 6: Electron Densities ($\rho$ in atomic units) and Laplacians ($\nabla^2\rho$) at the Bond Critical Points of Ionized iPrOPh, the Optimized Geometry with the O−$C_\alpha$ Bond Length Constrained to $r_{OC}$ = 2.6 Å, the Transition State for $\beta$-Elimination, and the Ion−Neutral Complex with $C_2$ Symmetry, Based on B3LYP/6-31G** Wave Functions**

| | O−$C_\alpha$/O−$H_\alpha$ | | O−$H_\beta$ | | $C_\beta$−$H_\beta$ | | $C_\alpha$−$C_\beta$ | |
|---|---|---|---|---|---|---|---|---|
| | $\rho$ | $\nabla^2\rho$ | $\rho$ | $\nabla^2\rho$ | $\rho$ | $\nabla^2\rho$ | $\rho$ | $\nabla^2\rho$ |
| iPrOPh$^{\bullet+}$ | 0.1986[a] | −0.2064[a] | no bcp | | 0.2795 | −0.9797 | 0.2550 | −0.6192 |
| constrained | 0.0177[a] | 0.0460[a] | 0.0166 | 0.0640 | 0.2572 | −0.8709 | 0.2871 | −0.7777 |
| transition state | no bcp | | 0.0421 | 0.1245 | 0.2259 | −0.6881 | 0.3028 | −0.8372 |
| [iPr$^+$ PhO$^\bullet$] | 0.0334[b] | 0.1176[b] | no bcp | | 0.2547 | −0.8325 | 0.2897 | −0.7869 |
| propene···HOPh$^{\bullet+}$ | no bcp | | 0.3090 | −1.7048 | 0.0313 | 0.0451 | 0.3397 | −0.9772 |

[a] O−$C_\alpha$ bond critical point; no bcp between $H_\alpha$ and oxygen. [b] O−$H_\alpha$ bond critical point; no bcp between $C_\alpha$ and oxygen.

with the C−O bond getting steadily weaker. At some point before the C−O bond distance reaches 2.6 Å a bifurcation occurs. Continued elongation leads to an ion−neutral complex (the higher energy pathway, represented by structure **B** in Figure 5). Alternatively, one of the $\beta$-hydrogens bonds to the oxygen, replacing the bond to carbon. In this lower energy pathway a new cyclic structure forms, but that ring opens prior to the syn transition state.

It is clear from the atoms-in-molecules analysis that the syn transition state does not possess cyclic structure. This conclusion may seem contrary to expectation, particularly since DFT calculations show $\beta$-elimination of HX from neutral alkyl halides to take place through bona fide cyclic transition states. For example, DFT optimizations of 2-fluoropropane and its transition state for HF expulsion show that the latter bears some resemblance to the syn ransition state from ionized iPrOPh. The calculated DFT electronic energy difference between reactant and transition state for HF elimination is 2.67 eV, with an unscaled zero-point energy correction of −0.20 eV. The net DFT activation barrier is thus not far from the reported $E_a$ of 2.35 eV, and the four-member transition state looks qualitatively like the cyclic model that has been proposed for it.[26] A ring point occurs in the transition state (there is none in the reactant), and a new bond critical point emerges between fluorine and the itinerant hydrogen without loss of any of the bond critical points of the reactant.

Weak bonds arise in a transition state either because new bonds are forming between previously nonbonded atoms or because formerly strong covalent bonds are loosening. The qualitative criterion of a weak bond is that the Laplacian of its electron density be $\nabla^2\rho > 0$ at the bond critical point. For instance, both bonds to fluorine have positive values of $\nabla^2\rho$ in the transition state for HF elimination from neutral 2-fluoropropane, indicating that the covalent C−F bond has weakened considerably while the H−F bond is developing.

Table 6 summarizes the changes that take place among the four atoms when ionized iPrOPh approaches the syn transition state. The bond between oxygen and the central carbon (O−$C_\alpha$) transforms from a covalent bond ($\nabla^2\rho < 0$) to a weak bond as it stretches to a bond length $r_{OC}$ = 2.6 Å. The comparatively slight elongation in going from there to the syn transition state (where $r_{OC}$ = 2.688 Å) leads to loss of bonding character. At the same time the weak bond between the itinerant hydrogen and the oxygen strengthens concomitant with a dramatic shortening of the distance between them ($r_{OH}$). At the top of the barrier the oxygen−hydrogen interaction has nearly the same $\rho$ and $\nabla^2\rho$ as the interaction between oxygen and the central hydrogen of the isopropyl cation in the [iPr$^+$ PhO$^\bullet$] complex.

The bond critical points for the $C_\alpha$−$C_\beta$ and $C_\beta$−$H_\beta$ bonds at $r_{OC}$ = 2.6 Å have $\rho$ and $\nabla^2\rho$ close to those of free isopropyl cation (whose bond critical points are virtually identical to those of iPr$^+$ within the ion−neutral complex). The atoms-in-molecules analysis concurs with our inference, based on calculated geometric changes, that $\beta$-elimination parallels bond heterolysis until just before the syn transition state, at which point an acidic hydrogen moves within bonding distance of the oxygen.

Experiment demonstrates that ionized sBuOPh and 3AmOPh lead to ion−neutral complexes in competition with $\beta$-elimination. By analogy to the computational results for iPrOPh$^{\bullet+}$, expulsion of $C_4H_{10}$ from ionized sBuOPh commences by elongation of a C−O bond, with development of cationic character in the alkyl group. At some critical extension the reaction branches among four pathways. At low internal energies, any one of three types of $\beta$-hydrogen interacts with the oxygen: the threo, the erythro, or one of the methyls. Statistically, the proportions should be 1:1:3, but experimentally the proportions are roughly 6:5:4, with no systematic variation with energy. In the fourth pathway, which dominates at higher internal energies, the bond extension continues past the point where $\beta$-hydrogen transfer takes place, and an ion−neutral complex forms.

How $\beta$-elimination distinguishes threo from erythro hydrogens remains to be discovered. Published mass spectrometric studies demonstrate that virtually all other *sec*-alkyl phenyl ethers exhibit a higher degree of stereospecificity than sBuOPh.[8] One plausible explanation might have supposed that formation of ion−neutral complexes masks a much higher selectivity, but the dissection presented here rules out such an interpretation for sBuOPh. While detailed computations have yet to be done, it seems likely that the energy gap between four-member transition states and the corresponding ion−neutral complexes for *sec*-alkyl cations with <3 carbons will be found to differ from the 0.2 eV calculated for iPrOPh$^{\bullet+}$, but an increasing fraction of complex formation may not necessarily correlate with an attenuation of stereospecificity. Further exploration of this competition may bring us closer to a predictive model for mass spectrometry.

## Conclusions

1. 2-Phenoxyalkanes exhibit ionization energies of 7.98 ± 0.02 eV, regardless of chain length (up to eight carbons) or deuterium substitution, but 3-phenoxyalkanes have ionization energies 0.04 eV lower.

2. Photoionization of sBuOPh yields ionized phenol via two competing pathways. Low photon energies ($h\nu \leq$ 9.8 eV) favor $\beta$-elimination from sBuOPh$^{\bullet+}$ via a syn transition state, which displays a measurable degree of stereospecificity (expelling *trans*-2-butene preferentially over *cis*) as well as regioselectivity (expelling *cis*-2-butene preferentially over 1-butene).

3. Higher photon energies increasingly favor the intermediacy of ion−neutral complexes, whose decomposition exhibits neither stereo- nor regiospecificity. Nevertheless, the proportion going by this pathway never becomes so great as to mask completely the specificity of $\beta$-elimination.

4. Theory (consistent with our interpretation of the experiments) suggests that ionized iPrOPh prefers to dissociate via the syn transition state (structure **A**) at the lowest internal energies. While structure **A** bears a resemblance to the transition states for vicinal elimination from neutral haloalkanes, it differs qualitatively from them, in that $\beta$-eliminations from neutral molecules pass through cyclic transition states, while the structure at the top of the barrier for the radical ion has acyclic topology.

5. DFT calculations indicate that formation of an ion−neutral complex (exemplified by structure **B**) from ionized iPrOPh has a barrier only 0.2 eV higher than the syn transition state. Therefore, we infer that propene elimination via **B** competes at higher internal energies, and we reject the $a = 0$ hypothesis, which posits that formation of ionized phenol takes place only via structure **A**.

6. The general mechanism for decomposition of ionized *sec*-alkyl phenyl ethers corresponds to the *y*-fixed model, in which deuterium exerts a small normal isotope effect for proton transfer from carbon to oxygen in an ion−neutral complex.

**Acknowledgment.** Support for this work was provided by NSF Grant CHE9522604, by the Australian Research Council, by the CNRS, and by a block grant of computing time from the San Diego Supercomputing Center/NPACI. The authors are grateful to Prof. L. J. Mueller for suggesting the Monte Carlo method for determining uncertainties and for implementing it using MATHEMATICA.

## References and Notes

(1) Fairweather, R. B.; McLafferty, F. W. *Org. Mass Spectrom.* **1970**, *4*, 221−224.

(2) Andlauer, B.; Ottinger, Ch. *J. Chem. Phys.* **1971**, *55*, 1471−1472.

(3) Traeger, J. C.; Morton, T. H. *J. Am. Chem. Soc.* **1996**, *118*, 9661−9668. The *m*/*z* 136 ($M^{\bullet+}$) curve in Figure 1 on p 9663 is enlarged ×5, which was omitted from the figure caption.

(4) Kondrat, R. W.; Morton, T. H. *Org. Mass Spectrom.* **1988**, *23*, 223−227.

(5) Schlosser, M.; Bossert, H. *Tetrahedron* **1991**, *52*, 6287−6292.

(6) Traeger, J. C. *Rapid Commun. Mass Spectrom.* **1996**, *10*, 119−122.

(7) Weddle, G. H.; Dunbar, R. C.; Song, K.; Morton, T. H. *J. Am. Chem. Soc.* **1995**, *117*, 2573−2580.

(8) Taphanel, M. H.; Morizur, J. P.; Leblanc, D.; Borchardt, D.; Morton, T. H. *Anal. Chem.* **1997**, *69*, 4191−4196.

(9) Hurzeler, H.; Inghram, M. G.; Morrison, J. D. *J. Chem. Phys.* **1958**, *28*, 76−82.

(10) Harnish, D.; Holmes, J. C. *J. Am. Chem. Soc.* **1991**, *113*, 9729−9734.

(11) Giner, J. L.; Buzek, P.; Schleyer, P. v. R. *J. Am. Chem. Soc.* **1995**, *117*, 12871−12872.

(12) Shaler, T. A.; Morton, T. H. *J. Am. Chem. Soc.* **1991**, *113*, 6771−6779.

(13) (a) Kondrat, R. W.; Morton, T. H. *Org. Mass Spectrom.* **1991**, *26*, 18−23. (b) Audier, H. E.; Morton, T. H. *Int. J. Mass Spectrom.*, in press.

(14) (a) Carneiro, J. W. de M.; Schleyer, P. v. R.; Koch, W.; Raghavachari, K. *J. Am. Chem. Soc.* **1990**, *112*, 4064−4066. (b) Sieber, S.; Buzek, P.; Schleyer, P. v. R.; Koch, W.; Carneiro, J. W. de M. *J. Am. Chem. Soc.* **1993**, *115*, 259−270.

(15) Dannenberg, J. J.; Goldberg, B. J.; Barton, J. K.; Dill, K.; Weinwurzel, D. H.; Longas, M. O. *J. Am. Chem. Soc.* **1981**, *103*, 7764−7768.

(16) (a) Becke, A. D. *J. Chem. Phys.* **1993**, *98*, 5648−5652. (b) Kohn, W.; Becke, A. D.; Parr, R. G. *J. Phys. Chem.* **1996**, *100*, 12974−12980.

(17) Rayón, V. M.; Sordo, J. A. *Theor. Chem. Acc.* **1998**, *99*, 68−70.

(18) (a) Chronister, E. L.; Morton, T. H. *J. Am. Chem. Soc.* **1990**, *112*, 133−139. (b) Morton, T. H. *Org. Mass Spectrom.* **1992**, *27*, 353−368. (c) McAdoo, D. J.; Morton, T. H. *Acc. Chem. Res.* **1993**, *26*, 295−302.

(19) Audier, H. E.; Morton, T. H. *J. Am. Chem. Soc.* **1991**, *113*, 9001−9003.

(20) Morton, T. H. *J. Am. Chem. Soc.* **1980**, *102*, 1596−1602.

(21) Burns, F. B.; Morton, T. H. *J. Am. Chem. Soc.* **1976**, *98*, 7308−7313.

(22) Morton, T. H. *Tetrahedron* **1982**, *38*, 3195−3243.

(23) Morton, T. H. In *Techniques for the Study of Ion−Molecule Reactions*; Farrar, J. M., Saunders: W. H., Jr., Eds.; Techniques of Chemistry XX; Wiley-Interscience: New York, 1988; pp 119−164.

(24) Aubry, C.; Holmes, J. L. *J. Phys. Chem. A* **1998**, *102*, 6441−6447.

(25) Bader, R. F. W. *Atoms in Molecules, a Quantum Theory*; Clarendon Press: Oxford, UK, 1994.

(26) Tschuikow-Roux, E.; Maltman, K. R. *Int. J. Chem. Kinet.* **1975**, *7*, 363−379.